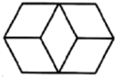

Optimizing the Parameters of diodes based on Gallium Sulfide Monolayer and Improving its Performance by Injecting Impurities and Introducing Defects

Mojtaba Moshtael[1], Maryam Nayeri[1*], Fatemeh Ostovari [2]

[1] *Department of Electrical Engineering, Yazd Branch, Islamic Azad University, Yazd, Iran.*
[2] *Department of Physics, Yazd University, Yazd, Iran.*
* *Corresponding Email: nayeri@iauyazd.ac.ir*

The gallium sulfide (GaS) monolayer is a potential two-dimensional semiconductor material with exceptional characteristics. GaS has a light gap of approximately 2.48 eV. However, it is indirect meaning the conduction band edge and finesse does not reside at a point in the wave vector's space. In this research, density functional theory-based calculations were used to study the diode properties of GaS nanowires. First, the parameters relevant to the analysis, such as the limit energy and the inverting spatial network, are optimized ,and then the GaS unit cell is optimized based on these parameters. The ideal grid vector and link length were used to complete the calculations. The electronic properties of the GaS transport channel with various impurities were investigated using state density calculations as well. The electronic transport of the GaS transport channel with impurities from different atoms was then estimated and examined using a current-voltage diagram. The diode characteristics of GaS nanowires were investigated using calculations based on modified density functional theory in this contribution. The GaS unit cell is optimized for this purpose by first optimizing the parameters connected with the computations, such as limit energy and inverted space meshing, and then employing these parameters. The best grid vector and connection length were utilized to continue the computations. Subsequently, the density of states calculations were used to investigate the electronic properties of the GaS transport channel with various impurities. Later, the electronic transport of the GaS transport channel with impurities from different atoms was calculated and investigated by calculating the current-voltage diagram.

Keywords: Gallium sulfide, Diode, Monolayer, Defects.

 © 2023 The Netherlands Press

1. Introduction

2D materials hold great promise for developing new nanodevices for future applications because of their fascinating electronic, mechanical, optical, and thermal properties, which can be attributed to their small dimensionality and quantum confinement effect. These nanostructures have novel properties that are superior to their solid counterparts [1]. 2D nanosheets with hexagonal structure such as graphene [2], a hexagonal boron nitride (h-BN) [3], silicene [4, 5], stanine [6], phosphors [7, 8] ,and transition metal dichalcogenides (TMDs) [9-12] have attracted extensive research efforts in recent years due to their excellent performance in nanoelectronic devices. The novel properties of these 2D materials hold promise for numerous industrial applications such as optoelectronics, photodetectors, catalysts, superconductors, and spintronic films [13]. However, the usefulness of these materials is limited by some shortcomings, such as the lack of a bandgap in graphene and the relatively low mobility in some TMDs [14]. This has motivated us to continue the search for other 2D materials that can demonstrate their properties and lead to an improvement in specific performance. Recently, another class of 2D materials, metal chalcogenides, was discovered and received much attention. These layer materials generally have the chemical formula MX, where M and X belong to group IIIA and IVA, respectively. GaS nanosheet has been successfully isolated by micromechanical cleavage technology [15, 16]. Monolayer gallium sulfide has been used in photodetectors, photoelectric devices, electrical sensors, devices that emit near blue light [16-19], and field-effect transistors (FETs). The mobility of 0.1 cm2 / V.S. was determined by David et al. [20] measured in ultra-thin GaS bottom-gate transistors. In addition, the piezoelectric coefficients of GaS monolayers are in the same order of magnitude as those of discovered two-dimensional (2D) piezoelectric materials such as boron nitride (BN) and MoS 2 monolayers [21].Gallium sulfide is an indirect bandgap semiconductor that interferes with optoelectronic devices that emit light and use photodetectors, and lasers. Since stresses are crucial in the development of band gaps in 2D structures [22-31], it would be exciting to investigate the influence of stresses on the band structure of GaS. If the energy difference between the indirect and direct band gaps is slight, a transition from indirect to direct bandgap is conceivable. Monochalcogenes are two-dimensional structures made of the thirteenth and sixteenth elements of the periodic table. The stoichiometry of these structures is MX, where M is an element from the thirteenth group and X is from the sixteenth group of the periodic table. The term chalcogen belongs to the elements of the sixteenth group, and since the unit cells of the structures in question are composed of the elements of this group and the elements of the thirteenth group in a ratio of 1 to 1, they are called monochalcogenes or single chalcogens. These compounds include GaS, GaSe, InS ,and InSe. The two-intermediate metal chalcogens, phosphorus, arsenic ,and monochalcogenes ,all have a bandgap. GaS also has a slight gap of about 2.48 eV, but its gap is indirect, which means that the edge of the conduction band and the finesse are not at one point in the space of the wave vector. In this paper, using calculations based on density functional theory, an attempt has been made to investigate the diode properties of GaS nanowires. For this purpose, the parameters related to the calculations ,such as the cut-off energy and the inverting space meshing, are first optimized, and then the GaS unit cell is optimized based on these parameters. Then, the optimal lattice vector and optimal

interconnect length were used to continue the calculations. Then, using the density of states calculations, the electronic properties of the GaS transport channel with different impurities were investigated. Then, by calculating the current-voltage diagram, the electronic transport of the GaS transport channel with impurities of different atoms was calculated and investigated.

2. The Theoretical Method

Quantum mechanics has improved our understanding of the structure and behavior of atoms, molecules, solids, and subatomic particles. Although classical physics is well adapted to explaining occurrences in the macroscopic realm, the study of all elements of the subatomic cosmos necessitates instruments that allow for more extensive and complicated computations. Density function theory may be used to calculate the quantum states of atoms, molecules, solids, and molecular dynamics. The one-electron theory is an approach used in computational density physics. This theory gives a method for solving the Schrodinger equation of a very particle-rich system and determining its ground state.

The one-electron theory is an approach used in computational density physics. This theory gives a method for solving the Schrodinger equation of a very particle-rich system and determining its ground state and ground state energy [21].

2.1Density functional theory

The single electron theory includes the Born-Oppenheimer and Hartry-Fock approximations. Following the definition of electron density and the Thomas-Fermi model, the Schrodinger equation converts a many-particle system into a single-particle equation and is one of the most critical methods. What exists in this theory is the density functional theory (DFT). This method is one of the most efficient computational methods for many-particle systems ,and this is due to its high computational efficiency, reduction in computational volume ,and good accuracy compared to other methods. The importance of DFT becomes even more apparent when we know that Cohen, one of the founders of the method, was awarded the Nobel Prize in Chemistry in 1998. Cohen and Sham considered a hypothetical device consisting of electrons that have no interaction, and eventually established equations that they used to calculate the ground-state properties of the device self-consistently. In density functional theory, the total energy is a combination of three sets: one is the fraction of the kinetic energy of the electrons, one is the fraction of the Coulomb energy due to the electrostatic interaction of all charged particles in the system, and the third is the exchange-correlation energy, which includes all interactions. The system consists of many particles. Among these sets, the exchange correlation energy fraction has an unknown form. It is not possible to find this energy in general. Therefore, approximation methods such as local density approximation (LDA) and generalized gradient approximation (GGA) should be used. The flowchart of self-consistent solution steps in DFT calculations is shown in Figure 1.

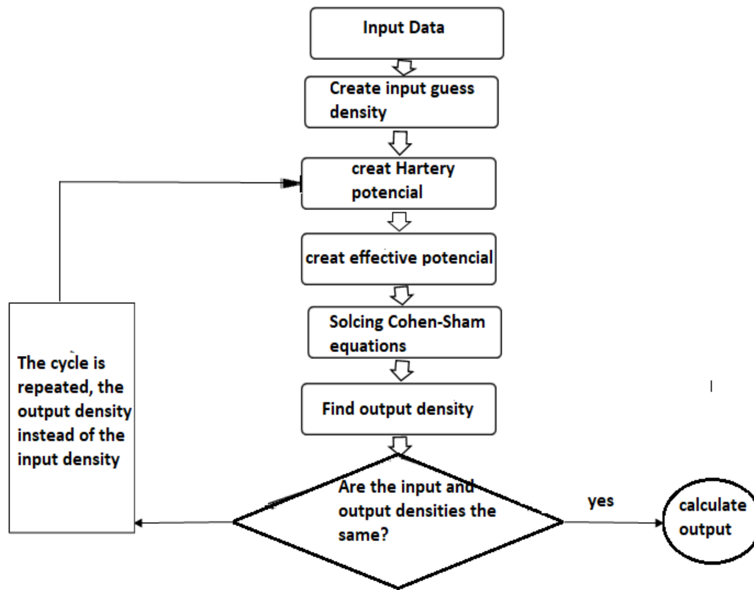

Figure 1. DFT calculations flow chart

Density functional theory deals with an n-electron system whose wave function is a variable n3-functional system. In this theory, all features of the electronic structure of the system, including the interaction of electrons in the external potential (potentials caused by nuclei), are determined by the density of the electron charge. Note that it is only a function of three variables, which reduces the computational volume. Density functional theory transforms the Schrodinger equation into a set of one-particle systems into a set of one-particle equations. These one-particle equations are known as Cohen-Sham equations, which depend only on the electron density [21].

The one-particle problem forms the study of atoms, molecules, solids, gases, liquids, etc. consisting of electrons and nuclei. Quantum mechanics can describe an interaction system of electrons and nuclei by the Schrodinger equation:

$$\hat{H}\Psi = E\Psi \quad (1)$$

Where E is the specific energy value, and the multiarticulate Hamiltonian operator (H̑) is given by Equation 2:

$$\hat{H} = \sum_{i=1}^{N=} -\hbar^2/_{2m}\nabla_i^2 + \sum_{i=1}^{N\,\text{Nare}} - \hbar^2/_{2M}\nabla_t^2 + \frac{1}{2}\sum_{i-j} e^2/|r_i - r_j| - \sum_{i,s} Z_i e2/|r_i - R_i| + \frac{1}{2}\sum_{\gamma=1} Z_i Zj^{e2}/|R_r - R| \quad (2)$$

In equation (2), the first and second parts are the kinetic energies of electrons and nuclei, and the last three parts are the interactions between electron-electron, electron-nucleus, and nucleus-nucleus, respectively. Planck's constant, m and M are the masses of electron and nucleus respectively, z_I is the atomic number of the 1st atom, e is the charge of the electron, r_i and R_I are the position of the 1st electron and the 1st nucleus.

Solving the Schrodinger equation is a very complex particle. To simplify the problem, the Born-Oppenheimer approximation is used, which states that nuclei are much heavier than electrons and move much slower than electrons. As a result, the motion of nuclei and electrons can be separated. It is assumed that the position of the atoms is fixed while the electrons move in the charge field of the nuclei. The general wave function can be divided into electronic and ionic wave functions. As a result, the Schrodinger equation for the electron part is given by Equation 3:

$$\widehat{\mathrm{H}}_e(r.R)\Psi_e = E_e\Psi_e(r.R) \quad (3)$$

The Hamiltonian electron operator is also expressed by Equation 4 below:

$$\hat{\mathrm{H}}_e = \sum_{i=1}^{N_e} - \hbar^2/_{2m}\nabla_i^2 + \frac{1}{2}\sum_{i\neq j} e^2/_{\left|r_i - r_j\right|} + \hat{V}_{ext} \quad (4)$$

In this equation; it is the potential that the nuclei exert on the electrons. Note that the interaction between the nuclei is entered as a parameter. Although the number of degrees of freedom of the system can be reduced by the Born-Oppenheimer approximation, the electron-electron interaction problem is still challenging to solve. Moreover, the electron wave function depends on the coordinates of all electrons. The number of electrons is much higher than the number of nuclei. As we will show below, it is more practical to use the density functional theory instead of the multi-particle wave function. Density functional theory requires fewer calculations and provides a good description of the electronic properties of the ground state of the system.

In density functional theory, the calculations are solved self-consistently. The computational steps of density functional theory can be expressed as follows: 1- Input data: The input data are the coordinates, the number of atoms ,and the total number of electrons. When the quasi-potential is used, we need to know its clear form, and when flat waves are used, we need to look at how the results depend on some critical parameters. For example, the number of points for the Brillouin domain. 2- Input density: In this step, we set the initial experimental density, which can be the overlap of atomic charge densities or comes from quasi-experimental calculations. 3- Generation of the Harter potential: here, we use the Equation of place ,which relates the second potential derivative to the charge density. 4- Generation of exchange potential: the exchange potential is calculated for the density entered. 5- Generation of the effective potential: this potential is obtained by adding the three components of the external exchange potential (V_ext), the Harter potential (V_Hartree) ,and the exchange-correlation potential (V_xc), and we show it with V_effect. 6- Solving the Cohen-Sham equations: At this stage, the Cohen-Sham equations are solved in both direct space and inverse space. 7- Determining the output density: by solving the Cohen-Sham equations, the output density is determined. 8- Testing the degree of convergence: In this phase, the difference between the input density and the output density is calculated. If it

is above a specific value, which is set in advance, the cycle must be repeated. However, if the difference is not significant, we have obtained the density of the ground-state.

3. Results and discussion

In this paper, an attempt is made to investigate the diode properties of GaS nanowires using calculations based on density functional theory. For this purpose, the parameters related to the calculations, such as the cut-off energy and the inverting space meshing, are first optimized, and then the GaS unit cell is optimized based on these parameters. Then, the optimal grating vector and interconnect length were used to continue the calculations.

Before performing the corresponding basic calculations and presenting their results, several parameters should be considered to increase the accuracy, decrease the computational cost, and increase the convergence speed. These parameters include the energy for cutting and meshing the inverted space.

3.1 Cut off energy

In computational codes, Cohen Sham single-particle wave functions are expanded according to flat base waves. Since the sentences of this expansion are gradually reduced for high-energy flat waves, these sentences can be considered zero for wave vectors whose energy exceeds a limit value called the cut-off energy. Moreover kept only the sentences whose kinetic energy is lower than the cut-off energy according to Equation (5). This limits the number of base functions in the expansion and reduces the computational volume:

$$\hbar^2/_{2\,m}\left|\vec{k}+\vec{G}\right|^2 \leq E_{cut} \qquad (5)$$

K and G are the wave functions and the coordinates of other symmetrical points relative to this point will be as follows respectively:

$$G = \left(\frac{2\pi}{\sqrt{3}a}, 0\right)$$

$$K = \left(\frac{2\pi}{\sqrt{3}a}, 0\right)$$

To obtain the optimal value of this parameter, all parameters except the cut-off energy were selected in an accurate and large input file to ensure that those parameters themselves do not cause errors, then change the cut-off energy at each step and Total energy was evaluated for different cut-off energies. The accuracy of energy calculation in the input files up to 0.001 eV was considered. Perdew-Burke-Ernzerhof (PBE) was used to increase the accuracy of the results of the exchange-correlation function.

The results (Figure 2) showed that the changes in total energy in terms of cut-off energy for the ,NC approximation after 600 eV have a uniform trend and energy changes are less than 0.001 eV. Therefore, this value was selected as the optimal parameter for the cut-off energy in the whole calculation process.

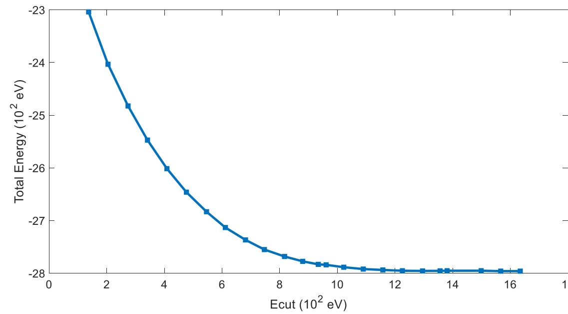

Figure 2. Graph of total energy in terms of cut-off energy (eV) for a GaS structure with quasi-potential NC.

3.2 Grid vector and number of K points in inverted space

In an infinite periodic solid, the number of atoms and electrons is huge. Since single-particle wave functions are spread over all solids, to calculate quantities such as charge density n (r) at the point r, a large number of wave functions that are finely distributed in space must be calculated. To be. Using Bloch's theorem, we can reduce the computational problem Ne ~(10^{23}) the number of single-particle wave functions ψ_i (r $\vec{}$) to the problem ψ_nk (r $\vec{}$) in the first Brillouin region for a limited number of bands.

$$\psi_n(\vec{k},\vec{r}+\vec{R}) = \psi_n(\vec{k},\vec{r})e^{(\vec{\imath k}.\vec{R})} \qquad (6)$$

Since the wave functions of the points k $\vec{}$ that are close together are very similar, the integration on all points k can be approximated by summing on a discontinuous set of points k. Although we need to know the wave functions for all k-points in the first Brillouin region, in practice it is sufficient to have wave functions in a limited number of these points. To integrate these points, we need to network the inverted space. The method in quantum espresso code is the Menkharest-Pack method [22]. Networking is done in the freedom and periodic directions of the structure, which is generally N × M × K.

These parameters are numbers (integers, N, M, K ≠0) to network the inverted space in different directions. For systems with three degrees of freedom ,such as heap systems (N × M × K), for two-dimensional networks (such as graphene) with two degrees of freedom in the direction a $\vec{}$ and b $\vec{}$ and the degree of restriction in the direction c $\vec{}$ (N × N × 1), for one-dimensional and quasi-one-dimensional structures such as nanotubes, nanowires ,and nanowires with a degree of freedom in the direction of c $\vec{}$ as 1 × 1 × N and for structures with three degrees of restriction in the direction of three a $\vec{}$, b $\vec{}$, c $\vec{}$, like molecules, are performed as 1 × 1 × 1, with point Γ at the center of the Brillouin region. The larger the cell and structure we are studying in real space, the smaller its inverted (Brillouin area) will be, and vice versa. Therefore, the smaller the inverted space, the fewer meshes ,and k points in the Brillouin area we need.

To obtain the optimal value of this parameter, all parameters except the inverted space mesh were selected in an accurate and large input file to ensure that those parameters themselves do not cause errors. The results of the previous step are used for the cut-off energy. Then the

inverted space meshing is changed in each step ,and the total energy for different inverted space meshing is investigated and reported in Figure (3).

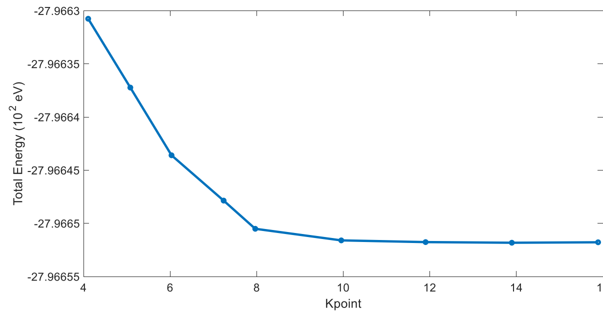

Figure 3. Total energy diagram in inverse space meshing for GaS structure with quasi-potential NC.

According to the obtained results (Figure 3), the changes of total energy in terms of inverse space meshing for NC approximation after meshing 8 × 1 8 1, have a uniform trend ,and energy changes are less than 0.001 eV. Therefore, 8×1×1 mesh was selected as the optimal parameter in all calculations.

3.3 Dimensional optimization of structures

After optimizing the parameters required to perform the calculations, the first action to be performed before examining the mechanical, electronic, and optical properties is to optimize the structure and position of the atoms. In this section, ionic dynamics and interatomic forces are studied by the Molecular Dynamics (MD) approach. There are different molecular dynamics methods for this, the BFGS method was used in the calculations, by which the atomic positions and positions are constantly changing, and in different states of force between them by the Hellman-Feynman method until The energy of the whole structure and system continues to be minimized for the position of atoms and ions. By optimizing the structure, atomic positions, equilibrium lattice constants, and the length of atomic bonds can be achieved in equilibrium.

The unit cell of a single-layer GaS structure has four atoms. The cubic unit cells of these structures are shown in Figure (4).

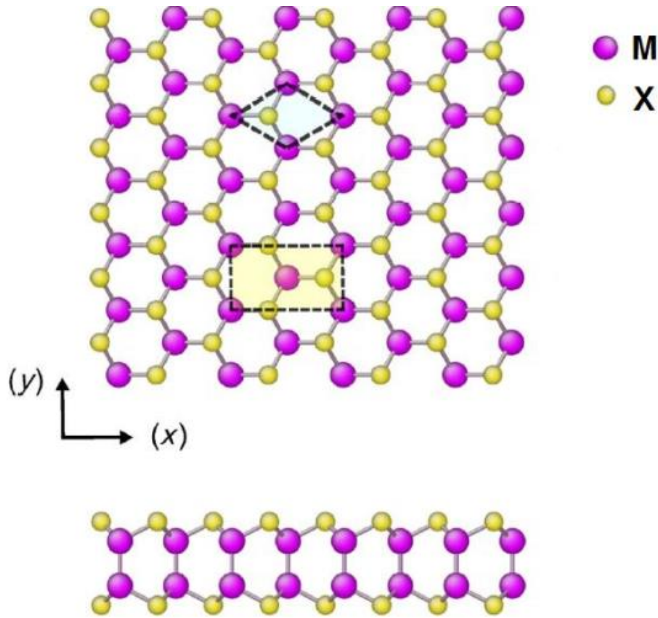

Figure 4. The unit cell has a two-dimensional GaS structure from top to bottom

After dimensional optimization, the new lattice vectors obtained for the GaS structure are reported in Table 1 and compared with previous theoretical results. The values calculated in this work are marked with an asterisk in the table.

case	Approximate	a (Å)	ref
GaS	DFT and LDA and GGA	3.43	This work
	LDA	3.58	[23]
	LDA	3.53	[24]
	GGA	3.48	[25]
	GGA	3.4	[26]

3.4 Electronic transport calculations of GaS structure

In the first step, the electronic properties and transport properties of two-dimensional GaS nanostructures have been studied. For this purpose, a section of the GaS two-dimensional structure is connected to two positive and negative electrodes (Figure 5). The electrodes are also made of GaS.

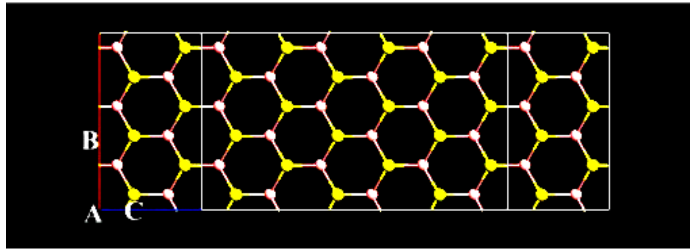

Figure 5. GaS transport channel structure and right and left electrodes connected to it made of GaS.

Using the DFT approach, a diagram of the density of the electronic states of the GaS transport channel is plotted (Figure 6). From this diagram, we find that the bandgap is a structure of 2.2 eV, which is consistent with the previous results ([23-27]). In addition, according to the diagram in Figure 6, it can be seen that the band gap in the GaS structure is not symmetric around the Fermi level and the Fermi level is closer to the edge of the capacity band, so the load carriers in this structure can be holes.

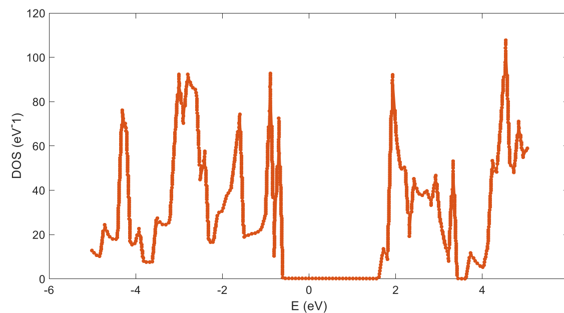

Figure 6. Electronic state density (DOS) diagram of GaS structure.

After examining the electronic properties of the GaS structure, the current-voltage diagram (I-V) related to this structure was calculated (Figure 7). At this stage, the flow through this GaS was investigated using the non-equilibrium Green function approach. This diagram is plotted in -5 to 5 + B bias to show GaS behavior in both positive and negative biases. According to Figure 7, it can be seen that among the voltages of -4 to +4, the behavior of GaS in positive and negative biases is similar ,and for more voltages of 2.2 V, it passes through the current transmission channel. The passing voltage (2.2 V) is the same as the 2.2 eV bandgap of the GaS structure, after which the valence electrons of the valence can be excited and pass through the bandgap to reach the conduction band and in electrical transmission.

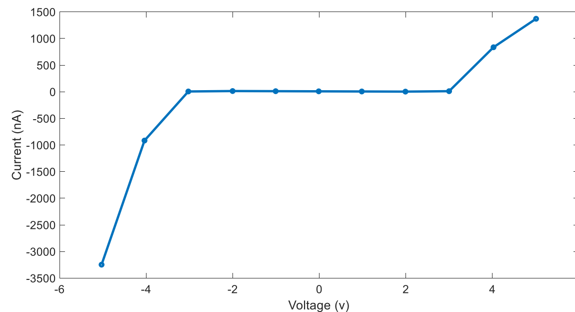

Figure 7. Current-voltage diagram of GaS structure at -5 V to 5V bias.

3.5 Defects by impurities in the structure of GaS

In order to investigate the effect of different defects or impurities (n-type impurities or p-type impurities) on the electronic properties of the GaS structure, we substituted atoms II, IV, V ,and VII instead of Ga and S atoms. Thus, an attempt has been made to design a diode based on a GaS structure using impurities of type n and p. Figure 8 shows the density of states calculated after the doping of the single atoms Ca, Mg, Ba and Sr instead of the Ga atom to the right of the transport channel. These atoms are group II elements that electronegatively tend to lose their electrons in the crystal lattice of the GaS structure and act as n-type impurities in the structure. Thus, by increasing the number of load carriers in the crystal lattice of the GaS transmission channel, they lead to faster and easier transmission of electrical current in the transmission channel. According to the diagram in Figure 8, after the doping of group II atoms instead of the Ga atom to the right of the GaS transport channel, the GaS semiconductor material has become a conductive material. Because after the doping of the single atoms Ca, Mg, Ba ,and Sr, peaks appear on the Fermi level in the state density diagram, which indicates the conduction of GaS. In this way, electrons can be quickly excited from the valence band under the influence of external voltage and transferred to the conduction band.

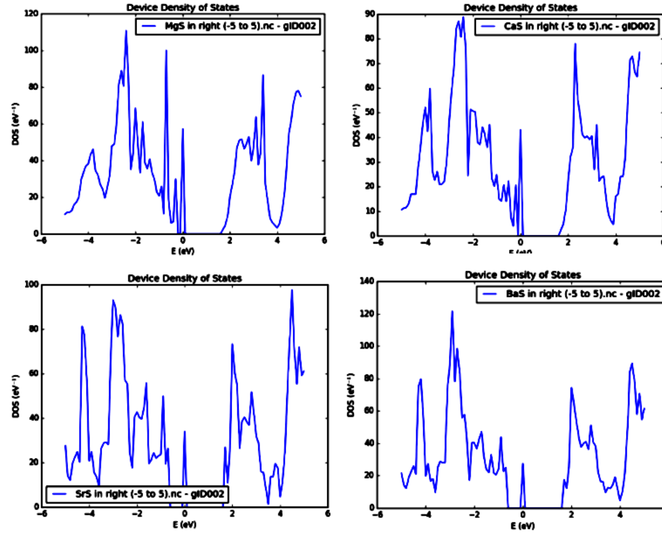

Figure 8. The density of states related to the structure of GaS after the doping of the single atoms Ca, Mg, Ba, and Sr instead of the Ga atom to the right of the transport channel.

In the next step, group IV atoms were used for impurities on the right side of the GaS transport channel instead of the Ga atom (Figure 9). After the doping of the single atoms Ca, Mg, Ba ,and Sr, instead of the Ga atom, as in group II atoms, a peak form is formed. The presence of an electron state on the Fermi level in the state density diagram allows electrons to transition from a valence level to a conduction level. Thus, with the doping of group IV atoms in the GaS transport channel, this material is conductive.

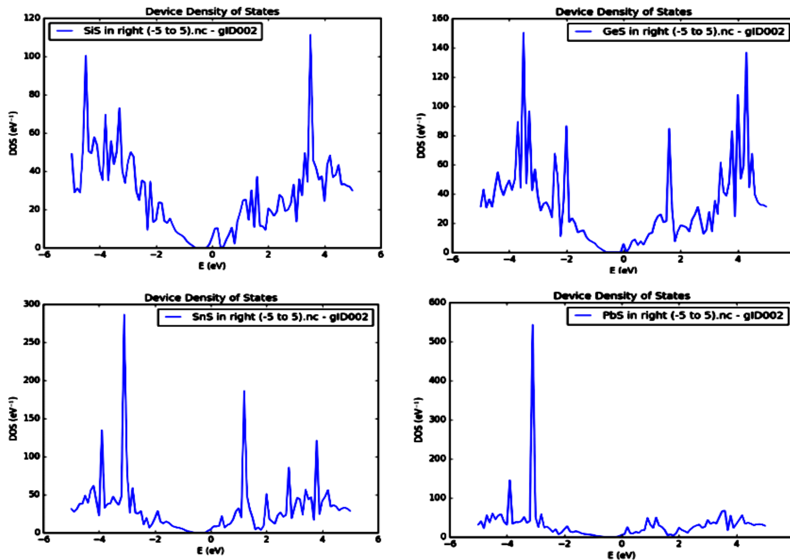

Figure 9. The density of states related to the structure of GaS after the doping of the single atoms Ge, Si, Pb ,and Sn instead of the Ga atom to the right of the transport channel.

In the next step, an attempt is made to change the properties with the impurities of group II atoms (Sr, Mg ,and Ca) on the left side of the transport channel and group IV atoms (Sn, Si ,and Ge) on the right side of the transport channel instead of Ga atoms. GaS transport channel electrons are calculated. The density of the calculated modes is shown in Figure 10. The calculated state densities show that in addition to the conduction channel of GaS under the influence of impurities of group II and IV atoms, many peaks are formed inside the GaS bandgap, which also increases the probability of band-to-band transitions inside. The light gap has increased. In the previous case, where only one atom of group II elements was doped to one side of the transport channel, the situation differed.

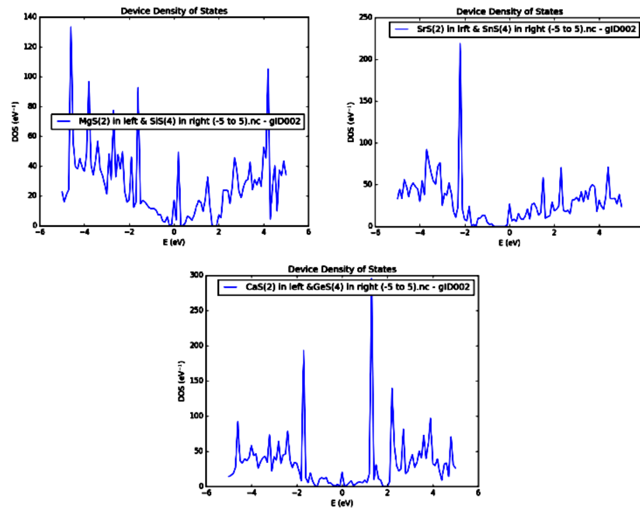

Figure 10. The density of states related to the structure of GaS after the doping of the single atoms Sn, Si ,and Ge instead of the Ga atom on the right side of the transport channel and the doping of the Sr, Mg ,and Ca atoms instead of the Ga atom on the left side of the transport channel.

In Figure 11, the density states of the GaS structure are calculated and plotted after the impurities of the single atoms Cl, Br, At, and I instead of the S atom to the right of the transport channel. With the doping of group VII atoms instead of S atoms in the GaS transport channel, states are created on the form level that leads to the conduction of the GaS structure.

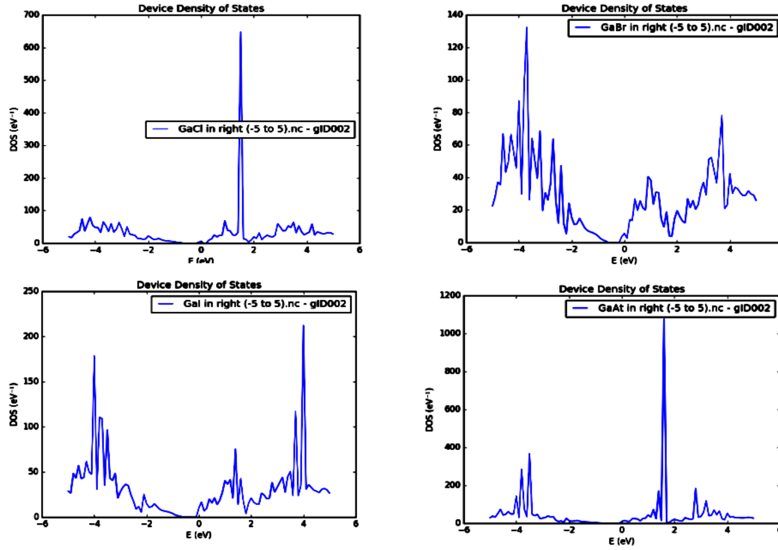

Figure 11. The density of states related to the structure of GaS after the doping of the single atoms Cl, Br, At ,and I instead of the S atom to the right of the transport channel.

In Figure 12, the density states of the GaS structure are plotted after the impurities of the single atoms Br, Cl, and At instead of the S atom to the right of the transport channel, and the impurities of the At, P, and Bi atoms instead of the S atom to the left of the transmission channel. Thus, the effect of impurities of group VII and V elements on the right and left of the transport channel on the electronic properties of the GaS transport channel was studied. According to the density diagram, the states drawn on the Fermi level have been created ,and these structures have also become conductive.

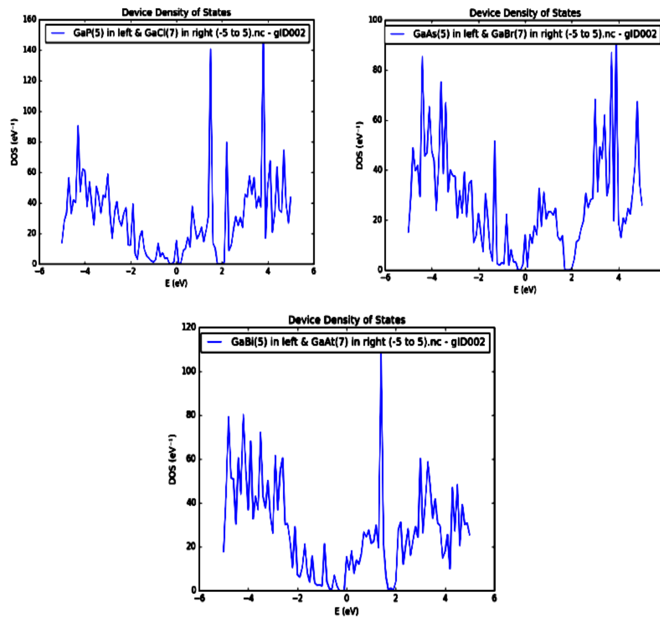

Figure 12. The density of states related to the structure of GaS after the doping of the single atoms Br, Cl, and At instead of the S atom on the right side of the transport channel and the doping of the As, P ,and Bi atoms instead of the S atom on the left side of the transport channel.

Then, in order to investigate the transport properties and the behavior of the GaS transport channel diode, a current-voltage diagram is drawn in the bias of -5 to +5 V. Figure 13 shows the current-voltage diagram of the GaS structure after the doping of the single atoms Ca, Mg, Ba and Sr instead of the Ga atom to the right of the transmission channel. What can be seen in the current-voltage diagram is that at positive bias, up to +3 V, the current was zero. In all these structures, after the voltage of +3 V, the current has gradually increased. The only difference is that the Mg atom is doped instead of the Ga atom. In this case, the trend of increasing current at +4 V suddenly decreases at +5 V from 7 μA to 2.5 μA. The maximum amount of current belongs to the Mg doping state, which at a voltage of +4, a current of 7 μA passes through the transmission channel. In reverse bias, in the two states of impurities Ba and Sr instead of the Ga atom, after a voltage of 2 V, the current gradually increases ,and the current intensity is almost equal to the direct bias mode. However, in the case of Ca ,and Mg impurities, the situation is different ,and the phenomenon of negative differential resistance (NDR) has occurred. In both cases, as soon as the reverse bias starts, the current is established in the transmission channel. But after 1V, the current starts to decrease and then increases again at 3V. Thus, the Ba and Sr atoms have little effect on the behavior of the transport channel for current rectification, but the Mg and Ca atoms can show NDR at negative bias.

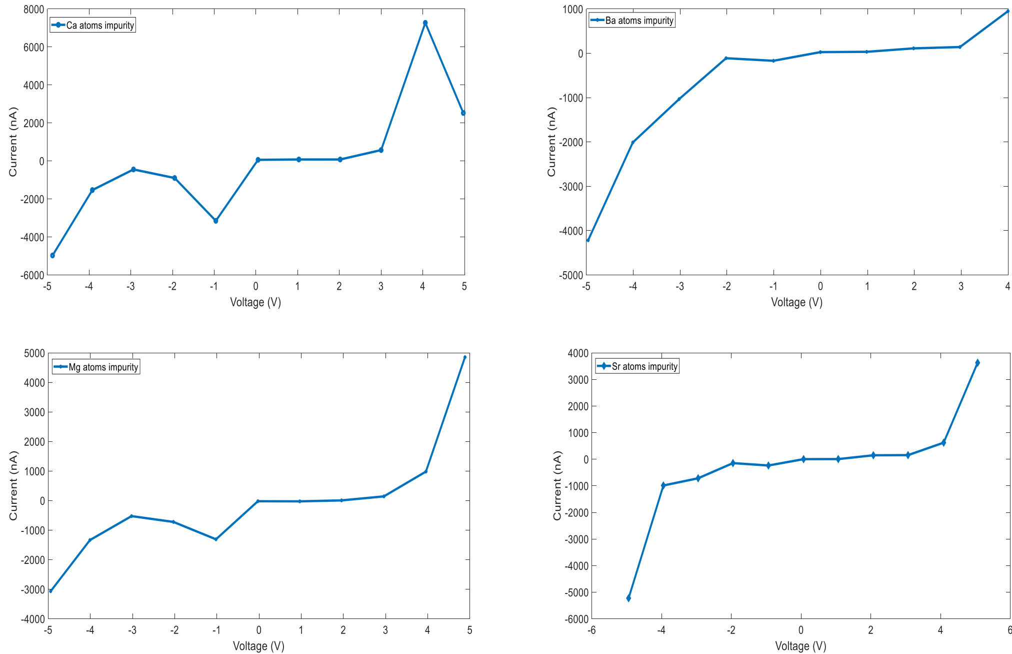

Figure 13. Current-voltage diagram of the GaS structure after doping single Ca, Mg, Ba ,and Sr atoms instead of Ga atoms to the right of the transport channel.

Current-voltage diagram of a GaS structure after doping of single atoms Sn, Si ,and Ge instead of Ga atom on the right side of the transmission channel and doping of Sr, Mg ,and Ca atoms instead of Ga atom on the left side of the transmission channel in Figure 14 given. Calculations show that indirect bias the current intensity is very low and in all three cases ,at +3 V NDR phenomenon has occurred. However, the current intensity indirect bias is not comparable to the current in reverse bias ,and more current in reverse bias is passing through the transmission channel. From the obtained diagrams, it is pretty clear that this type of doping has been able to have a significant effect on the smoothing characteristics of the transport channel. The impurities of the Sn, Si ,and Ge atoms, which belong to group IV, play the role of electron acceptor (p-type) to the system instead of the Ga atom to the right of the transport channel; And the impurities of the Sr, Mg, and Ca atoms instead of the Ga atom on the left of the transport channel play the role of the electron (n-type) in the transport channel. Thus, by creating an n-p type connection, the designed diode could smooth the current passing through the transmission channel. It should also be noted that with the doping of the Mg atom on the left and the Sr atom on the right of the transmission channel, the highest current in reverse bias passed through the transmission channel and was the best rectifier in this category. Most of the current passing through this transmission channel occurred in -5 V reverse bias with an intensity of 30 μA.

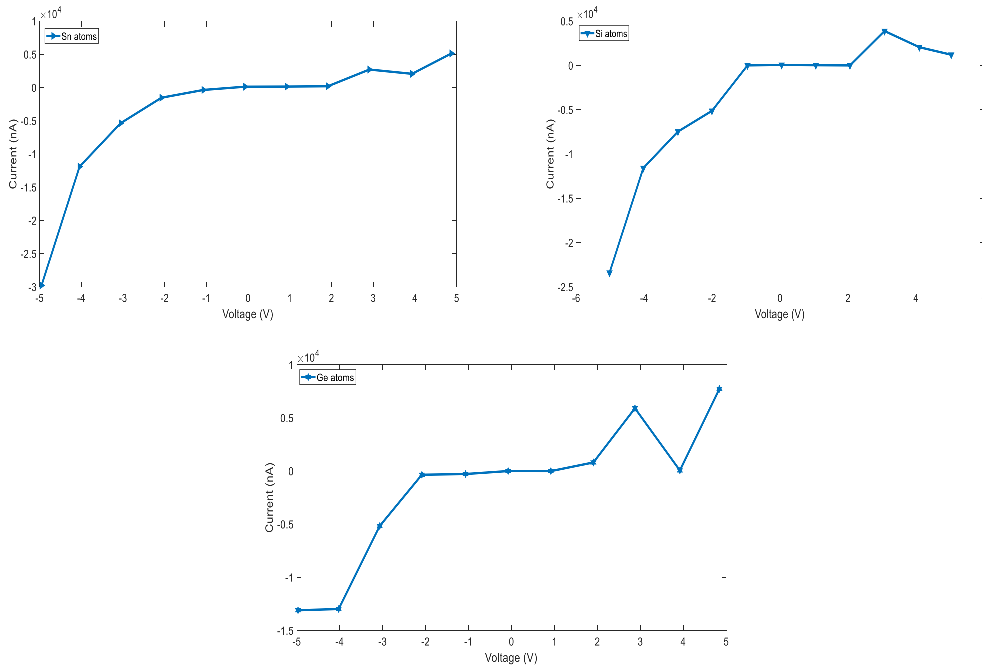

Figure 14. Current-voltage diagram of a GaS structure after doping of single Sn, Si ,and Ge atoms instead of Ga atoms on the right side of the transmission channel and impurities of Sr, Mg ,and Ca atoms instead of Ga atoms on the left side of the transmission channel

The impurities of the single atoms Ge, Si, Pb ,and Sn instead of the Ga atom on the right side of the transport channel could not lead to a definite rectification in the transport channel. In this type of pollution, indirect bias, after a voltage of +1 V, current flows in the system, and after a voltage of 2 to 3 V, the current decreases ,and the NDR phenomenon occurs. At a voltage of +4 V, the current is completely cut off ,and then, with a gradual increase in voltage, the current is restored in the system. In contrast, in reverse bias, after a voltage of 2 V, the current is established and has increased in a quasi-ohmic manner. The only thing that has happened in the reverse bias of the NDR phenomenon is that the Ge atom is doped instead of the Ga atom. In this case, the NDR phenomenon has occurred at -3 to 4 V. Among these structures, most of the current flow was in reverse bias after the doping of the Si atom instead of Ga, which reached more than 16 µA at 5V.

4. Conclusions

In this paper, using calculations based on modified density functional theory, an attempt has been made to investigate the diode properties of GaS nanowires. For this purpose first, by optimizing the parameters related to the calculations such as cut-off energy and inverting space meshing and then using these parameters, the GaS unit cell is optimized. Then the optimal grid vector and the optimal link length were used in to continue the calculations. Then, using state density calculations, the electronic properties of GaS transport channels with different impurities were investigated. Then, by calculating the current-voltage

diagram, the electronic transport of GaS transport channel with impurities of different atoms was calculated and investigated.

The DFT approach calculates the electronic properties and transport characteristics of a pure and contaminated GaS transport channel. The graph of the density of electron states related to the GaS transmission channel showed that the bandgap of the structure is 2.2 eV. In addition, the bandgap in the GaS structure is not symmetric around the Fermi level ,and the Fermi level is closer to the edge of the capacity band, so the load carriers in this structure can be cavities. Then, by plotting the current-voltage diagram, it was observed that among the voltages of -4 to +4, the behavior of GaS in positive and negative biases is similar ,and for more voltages, 2.2 V passes through the current transmission channel. The passing voltage (2.2 V) is the same as the bandgap 2.2 eV of the GaS structure, after which the valence electrons of the valence can be excited and pass through the bandgap to reach the conduction band and in electrical transmission. Participate. In order to investigate the effect of different impurities (n-type impurities or p-type impurities) on the electronic properties of the GaS structure, atoms of groups II, IV, V ,and VII were substituted instead of Ga and S atoms. Thus, an attempt has been made to design a diode based on a GaS structure using impurities of type n and p. After the impurities of the atoms of groups II, IV, V and VII instead of the Ga and S atoms in the GaS transport channel, the semiconductor material GaS has become a conductive material. Because after the doping of these atoms, peaks appear on the Fermi level in the state density diagram, which indicates the conduction of GaS. Then, in order to investigate the transport properties and the behavior of the GaS transport channel diode, a current-voltage diagram is drawn in the bias of -5 to +5 V. The Ba and Sr atoms have little effect on the behavior of the transport channel for current rectification, but the Mg and Ca atoms can exhibit NDR at negative bias. When the Mg atom is doped instead of the Ga atom, the current increase in current at +4 V suddenly decreases from + 7 μA to 2.5 μA at +5V. The maximum amount of current belongs to the Mg doping state, which at a voltage of +4, a current of 7 μA passes through the transmission channel. The impurities of the Sn, Si ,and Ge atoms, which belong to group IV, play the role of electron acceptor (p-type) to the system instead of the Ga atom to the right of the transport channel; And the impurities of the Sr, Mg, and Ca atoms instead of the Ga atom on the left of the transport channel play the role of the electron (n-type) in the transport channel. Thus, by creating an n-p type connection, the designed diode could smooth the current passing through the transmission channel. It should also be noted that with the doping of the Mg atom on the left and the Sr atom on the right of the transmission channel, the highest current in reverse bias passed through the transmission channel and was the best rectifier in this category. Most of the current passing through this transmission channel occurred in -5 V reverse bias with an intensity of 30 μA.

References

[1] Wang Q H, Kalantar-Zadeh K, Kis A, Coleman J N and Strano M S 2012 Electronics and optoelectronics of two-dimensional transition metal dichalcogenides Nat. Nanotechnol. 7 699

[2] Nayeri M, Moradinasab M and Fathipour M 2018 The transport and optical sensing properties of MoS2, MoSe2, WS2 and WSe2 semiconducting transition metal dichalcogenides Semicond. Sci. Technol. 33 025002

[3] Yan Z, Yoon M and Kumar S 2018 Influence of defects and doping on phonon transport properties of monolayer MoSe2 2D Mater. 5031008

[4] Li S L, Tsukagoshi K, Orgiu E and Samorì P 2016 Charge transport and mobility engineering in two-dimensional transition metal chalcogenide semiconductors Chem. Soc. Rev. 45 118–51

[5] Nayeri M and Taheri H 2019 The influence of impurity on the electronic properties of WS2 single layer 2019 27th Iranian Conf. on Electrical Engineering (ICEE) (Piscataway, NJ) (IEEE) pp 224–7

[6] Manzeli S, Ovchinnikov D, Pasquier D, Yazyev O V and Kis A 2017 2D transition metal dichalcogenides Nature Reviews Materials 217033

[7] Nayeri M, Fathipour M and Goharrizi A Y 2016 The effect of uniaxial strain on the optical properties of monolayer molybdenum disulfide J. Phys. D: Appl. Phys. 49 455103

[8] Trainer D J, Zhang Y, Bobba F, Xi X, Hla S W and Iavarone M 2019 The effects of atomic-scale strain relaxation on the electronic properties of monolayer MoS2 ACS nano 13 8284–91

[9] Nayeri M and Fathipour M 2018 A numerical analysis of electronic and optical properties of the zigzag MoS2 nanoribbon under uniaxialstrain IEEE Trans. Electron Devices 65 1988–94

[10] Novoselov K S, Mishchenko A, Carvalho A and Neto A C 2016 2D materials and van der Waals heterostructures Science 353 aac9439

[11] Yang S, Jiang C and Wei S H 2017 Gas sensing in 2D materials Applied Physics Reviews 4 021304

[12] Jappor H R 2017 Electronic structure of novel GaS/GaSe heterostructures based on GaS and GaSe monolayers Physica. B 524 109–17

[13] Hu P, Wen Z, Wang L, Tan P and Xiao K 2012 Synthesis of few-layer GaSe nanosheets for high performance photodetectors ACS Nano 6 5988–94

[14] Late D J, Liu B, Luo J, Yan A, Matte H R, Grayson M, Rao C N R and Dravid V P 2012 GaS and GaSe ultrathin layer transistors Adv. Mater. 24 3549–54

[15] Lei S, Ge L, Liu Z, Najmaei S, Shi G, You G, Lou J, Vajtai R and Ajayan P M 2013 Synthesis and photoresponse of large GaSe atomic layers Nano Lett. 13 2777–81

[16] Demirci S, Avazlı N, Durgun E and Cahangirov S 2017 Structural and electronic properties of monolayer group III monochalcogenides Phys. Rev. B 95 115409

[17] Ma Y, Dai Y, Guo M, Yu L and Huang B 2013 Tunable electronic and dielectric behavior of GaS and GaSe monolayers Phys. Chem. Chem. Phys. 15 7098–105

[18] Yagmurcukardes M, Senger R T, Peeters F M and Sahin H 2016 Mechanical properties of monolayer GaS and GaSe crystals Phys. Rev. B 94 245407

[19] Chen H, Li Y, Huang L and Li J 2015 Influential electronic and magnetic properties of the galliumsulfide monolayer by substitutional doping J. Phys. Chem. C 119 29148–56

[20] Li W and Li J 2015 Piezoelectricity in two-dimensional group-III monochalcogenides Nano Research 8 3796–802

[21] Y. Zhou, S. Li, W. Zhou, X. Zu, and F. Gao, "Evidencing the existence of intrinsic half-metallicity and ferromagnetism in zigzag gallium sulfide nanoribbons," Scientific reports, vol. 4, p. 5773, 2014.

[22] H. J. Monkhorst and J. D. Pack, "Special points for Brillouin-zone integrations," Physical review B, vol. 13, no. 12, p. 5188, 1976.

[23] B. P. Bahuguna, L. K. Saini, R. O. Sharma, and B. Tiwari, "Hybrid functional calculations of

electronic and thermoelectric properties of GaS, GaSe, and GaTe monolayers," Physical Chemistry Chemical Physics, vol. 20, no. 45, pp. 28575-28582, 2018.

[24] T. Chen et al., "Ultrathin All-2D Lateral Graphene/GaS/Graphene UV Photodetectors by Direct CVD Growth," ACS Applied Materials & Interfaces, 2019.

[25] B. Zhou et al., "A type-II GaSe/GeS heterobilayer with strain enhanced photovoltaic properties and external electric field effects," Journal of Materials Chemistry C, vol. 8, no. 1, pp. 89-97, 2020.

[26] B. Chitara and A. Ya'akobovitz, "Elastic properties and breaking strengths of GaS, GaSe and GaTe nanosheets," Nanoscale, vol. 10, no. 27, pp. 13022-13027, 2018.

[27] A. Fleurence, R. Friedlein, T. Ozaki, H. Kawai, Y. Wang, and Y. Yamada-Takamura, "Experimental evidence for epitaxial silicene on diboride thin films," Physical review letters, vol. 108, no. 24, p. 245501, 2012.